Available online at www.sciencedirect.com
ScienceDirect
Journal of Crystal Growth 310 (2008) 959–965
JOURNAL OF CRYSTAL GROWTH
www.elsevier.com/locate/jcrysgro

Lattice parameters of bulk GaN fabricated by halide vapor phase epitaxy

V. Darakchieva[a,*], B. Monemar[a], A. Usui[b], M. Saenger[c], M. Schubert[c]

[a]*Department of Physics, Chemistry and Biology, Linköping University, S-581 83 Linköping, Sweden*
[b]*R&D Division, Furukawa Co. Ltd., Tsukuba, Ibaraki 305-0865, Japan*
[c]*Department of Electrical Engineering, University of Nebraska, Lincoln, NE 68588, USA*

Available online 2 January 2008

Abstract

The lattice parameters of low-defect density undoped bulk GaN fabricated by halide vapor phase epitaxy (HVPE) and removal of the substrate are precisely determined using high-resolution X-ray diffraction. The obtained values, $c = 5.18523$ Å and $a = 3.18926$ Å are compared with the lattice parameters of free-standing HVPE-GaN from different sources and found to be representative for state-of-the-art undoped HVPE bulk GaN material. A comparison with bulk GaN fabricated by the high pressure technique and homoepitaxial GaN layer is made, and the observed differences are discussed in terms of their free-electron concentrations, point and structural defects.

PACS: 81.05.Ea; 61.10.Nz; 61.82.Fk

Keywords: A1. GaN bulk; A1. Lattice parameters; A1. High-resolution x-ray diffraction; A1. Point and extended defects; B3. Hydride/Halide vapor phase epitaxy

1. Introduction

Despite the remarkable progress in the III-nitride research and technology, some basic bulk properties of GaN and related materials remain uncertain and further technological developments are in need [1,2]. One of the main obstacles impeding further progress in the field is the lack of native substrates in the growth process and consequent difficulties to prepare strain-free material. Substantial efforts have been directed to the fabrication of bulk GaN and AlN using high-pressure (HP) growth from solution [3], sodium melt [4] or in supercritical ammonia [5] and sublimation epitaxy [6]. An alternative approach is the growth of thick GaN layers on 2 in substrates by halide vapor phase epitaxy (HVPE), which provides high quality material at low cost, combined with separation of the substrates at a certain stage [7,8]. Recent developments in the HVPE growth of GaN [9–12] have enabled the fabrication of high quality large diameter single-crystalline free-standing (FS) GaN substrates and provide the possibility to explore the bulk fundamental properties of GaN.

Fundamental properties of semiconductor materials, like electronic band structure, band gap energy, dynamical and elastic properties, etc., are directly related to the material lattice parameters. The knowledge of the material lattice parameters is therefore essential from a physical point of view and also for device engineering. This issue is presently of particular importance for III-nitride materials and related technology since the reported lattice parameters of GaN show unusually large fluctuations and it is difficult to determine the *intrinsic* unstrained values [13]. In principle, the lattice parameters of GaN might be affected by: (i) incorporation of impurities; (ii) presence of native point defects, (iii) presence of extended and 3D defects, (iv) growth induced and thermally induced strain in the case of heteroepitaxial layers. The incorporation of impurities has at first place the purely size effect on the lattice parameters related to the lattice relaxation around the impurity atom, and secondly the electronic effect related to the deformation potentials as a result of placing free-carriers in the

*Corresponding author. Tel.: +46 13 282629; fax: +46 13 142337.
E-mail address: vanya@ifm.liu.se (V. Darakchieva).

0022-0248/$ - see front matter © 2007 Elsevier B.V. All rights reserved.
doi:10.1016/j.jcrysgro.2007.11.130

conduction or valence bands [14]. Recent theoretical studies predict that incorporation of Si and Be causes contraction of the lattice, while O and Mg cause expansion [14]. There is no reliable theoretical or experimental evidence on the effect of the most abundant native point defects in GaN, i.e. Ga and N vacancies and their complexes with dopant impurities. Extended defects like dislocations may affect directly the lattice parameters, but evaluation is usually very difficult, since some types of dislocations may interact with point defects forming complex defects. Further, precipitates and complex pyramidal defects in bulk crystals [15,16] may influence the lattice parameters directly via the size effect and through the different thermal expansion coefficients compared to the host lattice, which can cause contraction or expansion of the matrix during cooling down. Finally, in the case of HVPE FS GaN substrates some residual strain may be present as a result of the heteroepitaxial nature of the growth. This small residual strain, often demonstrated by a bending of the FS GaN materials [17,18], was shown to vary depending on the thickness of the FS substrate and the particular nucleation scheme used [19].

The lattice parameters of HP bulk GaN and homoepitaxial GaN have been extensively studied [15,20–22]. The GaN crystals grown by the HP method exhibit a very low dislocation density (10^2–$10^4\,cm^{-2}$), but typically show a high free-electron concentration $>10^{19}\,cm^{-3}$ (related to high O incorporation) [20,21]. Such a high free-electron concentration was predicted to produce measurable changes in the GaN lattice parameters [14]. Indeed, measured lattice parameters of HP bulk GaN crystals show a difference of 0.0009 and 0.002 Å from the a and c lattice parameters of a homoepitaxially grown GaN layer with a free-electron concentration of $\sim10^{17}\,cm^{-3}$ [15]. Therefore, although being very close, the lattice parameters of HP bulk GaN still deviate somehow from the *intrinsic* strain-free values. This also causes the homoepitaxial GaN layer grown on top of such bulk GaN material to be strained. On the other hand, lattice parameters of bulk GaN fabricated by HVPE and subsequent substrate removal, showing free-carrier concentration $\leqslant10^{17}\,cm^{-3}$, have only been reported for samples with limited thicknesses [19]. The reported lattice parameters of HVPE GaN substrates scatter slightly, and for some cases they may still be affected by bending, residual strain, etc. [18,19,23]. The large variation in the reported lattice parameters of heteroepitaxial GaN layers and FS material may be affected by differences in the measuring procedure as well.

In this work we report on a precise determination and comparative analysis of the lattice parameters of 2 mm-thick low-defect density undoped bulk GaN fabricated by HVPE at Furukawa Co., Japan.

2. Experimental

The $15\times10\,mm^2$ bulk sample was grown along the GaN [0 0 0 1] direction using a facet-initiated lateral epitaxial overgrowth technique up to a thickness of about 2 mm, followed by a removal of the sapphire substrate [12]. The Ga-face is as-grown while the N-face was chem-polished.

In order to assess the free-carrier concentration and phonon parameters in the bulk GaN we have performed room-temperature infrared spectroscopic ellipsometry (IRSE) measurements in the spectral range of 350–$1500\,cm^{-1}$ with a spectral resolution of $2\,cm^{-1}$, and at 60° and 70° angles of incidence. The IRSE data were modeled using a two-phase model: ambient/bulk GaN accounting for polar phonon contribution and a possible contribution from free-carriers to the dielectric function [24,25]. Further details about the IRSE experiment and data analysis can be found in Refs. [24,25] and references therein.

Micro-Raman measurements were carried out at room temperature on a confocal Jobin-Yvon spectrometer equipped with a CCD detector and with a home-made Raman system with high-power, large aperture Raman head and a Jobin-Yvon spectrometer unit. The 514.5 and 488 nm lines of an Ar^+ laser were used for excitation and the spectral resolution was about $1\,cm^{-1}$. The experiment was conducted in $z(xx)\bar{z}$ backscattering configuration with the z-direction oriented along the c-axis, which allows the detection of the GaN E_2 and A_1(LO) modes [26]. Further cross-section Raman backscattering spectroscopy is carried out in $x(z,z)\bar{x}$ and $x(z,y)\bar{x}$ configurations allowing the detection of the A_1(TO), E_1(TO), E_2 and quasi-longitudinal QLO phonon modes [26].

High-resolution X-ray diffraction (HRXRD) and reciprocal space mapping (RSM) were performed at room temperature using a Philips triple axis diffractometer following the alignment procedures described in Ref. [27]. The measurements were performed with both (i) a parabolic graded multilayer mirror collimator, followed by a channel-cut 2-bounce Ge(2 2 0) monochromator on the primary side and an asymmetric 2-bounce Ge(2 2 0) analyzer crystal giving a resolution of 30 arcsec; and (ii) a four-crystal monochromator in a Ge(2 2 0) configuration and a channel cut analyzer with 12 arcsec acceptance in triple axis setup.

Cathodoluminescence (CL) imaging and spectroscopy were performed at a temperature of 4.6 K and with electron beam accelerating energy of 10 kV in a Leo 1500 Gemini scanning electron microscope with a MonoCL2 CL attachment (Oxford Research Instruments).

3. Results and discussion

3.1. Free-carrier concentration and structural quality

Fig. 1 shows experimental and best-fit model calculated IRSE Ψ spectra from the Ga-face of the bulk HVPE-GaN. The polar phonon parameters and the free-electron concentration, N_e are extracted from the best-match modeling to the experimental IRSE data. As a result sharp phonon lines with broadening parameters $\leqslant2\,cm^{-1}$ were

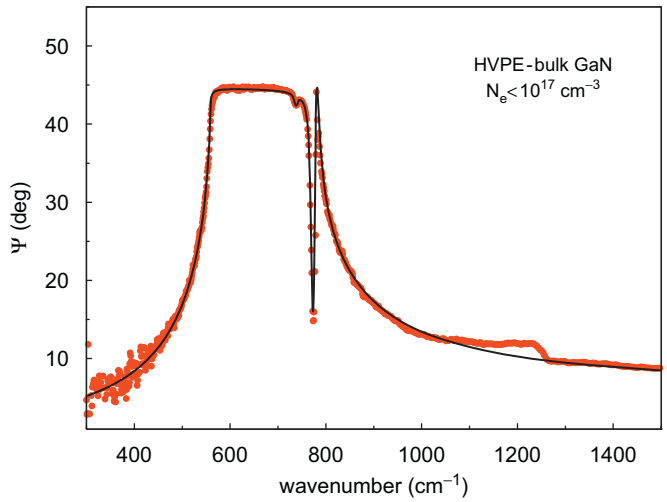

Fig. 1. Experimental (dots) and calculated (line) IRSE Ψ spectra of the 2 mm-thick HVPE bulk GaN at 70° angle of incidence.

revealed and a free-electron concentration, N_e, to be below the detection limit of the IRSE technique of 1×10^{17} cm^{-3} was determined. The low carrier concentration in the bulk GaN is further confirmed by Raman scattering spectroscopy. The allowed E_2 and the uncoupled A_1(LO) phonons are detected in the $z(xx)\bar{z}$ spectra (not shown here) for both Ga- and N-faces. Fig. 2 shows $x(z,y)\bar{x}$ cross-sectional Raman spectra, taken in different spots along the bulk GaN, revealing the allowed E_1(TO), some leakage of the A_1(TO) mode due to non-optimal polarization detection and the symmetry-forbidden but Fröhlich allowed quasi-longitudinal (QLO) phonon [28]. The QLO phonon frequency is very close to that of pure E_1(LO) phonon and may contain a small component with A_1 symmetry. All measurements have been performed at multiple locations of the bulk HVPE-GaN sample. In all cases the observed E_1(LO) (QLO) and A_1(LO) do not couple to plasmon excitations (see Fig. 2) indicating that the free-electron concentration remains below 1×10^{17} cm^{-3} across the thickness of the bulk sample [29]. Further, the frequencies and broadening parameters of the different phonons are constant (within the experimental errors) both across the sample surface and the thickness, indicating that there is no variation of strain and implying good spatial and in-depth uniformity.

Furthermore, low temperature (2 K) photoluminescence (PL) measurements reveal sharp dominant lines associated with the recombination of the A exciton bound to O and Si donors with full width at half maximum (FWHM) less than 0.3 meV. The latter evidences the low background donor concentration ($<5 \times 10^{16}$ cm^{-3}) and confirms the high structural quality of the material. This is also supported by the observation of sharp two-electron transitions in the PL spectra [30].

Fig. 3 shows an RSM around the GaN 105 reciprocal lattice point from the Ga-face of the bulk HVPE-GaN (Fig. 3a) in comparison with the Ga-face of a 300 μm

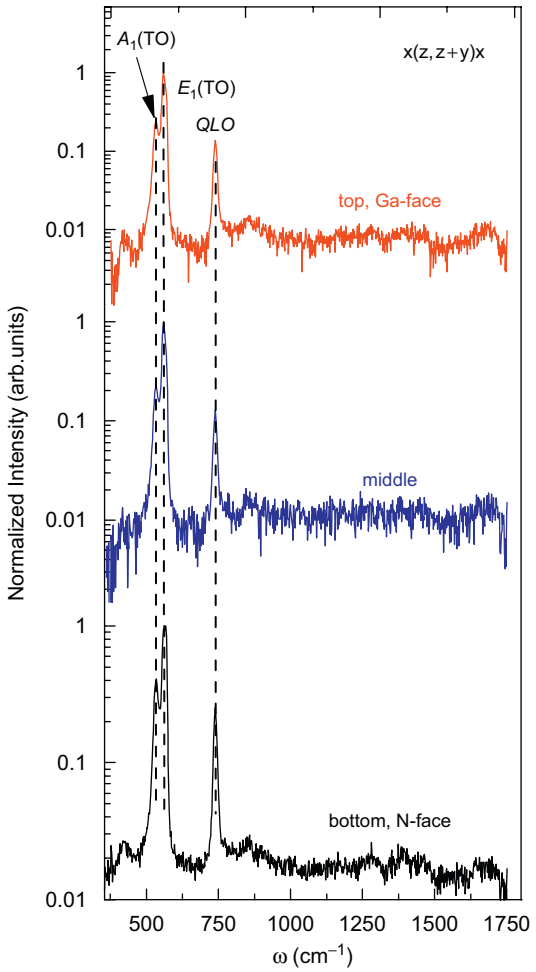

Fig. 2. Raman spectra in $x(z,z+y)\bar{x}$ configuration taken at three different spots along the cross-section of the bulk GaN sample.

HVPE FS GaN (grown at Lumilog SA) after laser-lift-off from a sapphire substrate (Fig. 3(b)). The two RSMs have the elliptical shape typical for III-nitrides with a mosaic structure. The RSM from the bulk HVPE GaN is considerably narrower in the ω direction compared to the FS layer, as a result of minimizing both curvature and dislocation density. An upper limit for the screw type of dislocations was estimated from the tilt angle (extracted from the Williamson–Hall plots) [31] to be below 3×10^6 cm^{-2}. Fig. 4 shows a panchromatic CL image of the bulk HVPE-GaN sample revealing a number of dark spots. The dark contrast in the CL map can be related to a strong non-radiative recombination around screw and mixed type of dislocations [32]. The estimated density of screw and mixed type of dislocations (Fig. 4) of $6.8 \pm 0.6 \times 10^6$ cm^{-2} is in good agreement with the HRXRD results. The high crystallographic quality and low dislocation density is manifested in very narrow rocking curves of symmetric and asymmetric peaks. For instance, the Ga-face 006 and 205 rocking curves are about 30 and 25 arcsec, respectively (Table 1). Such high-quality, low-defect density material is therefore the prime choice for

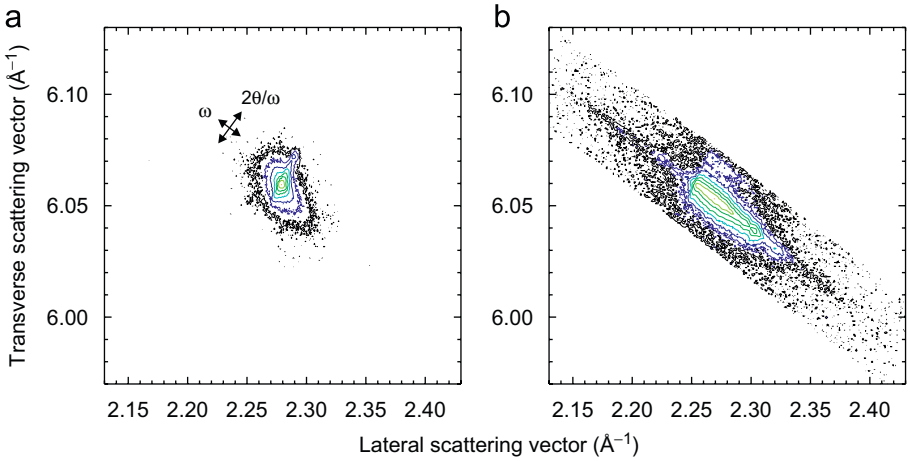

Fig. 3. Reciprocal space maps around the GaN 105 reciprocal lattice point of (a) the 2 mm-thick HVPE bulk GaN and (b) 300 μm-thick HVPE-GaN free-standing separated by laser lift-off from the substrate. The RSMs are normalized to the maximum intensity and the same seven contour levels (from 0.0001 to 1) equidistant in log scale are used in (a) and (b).

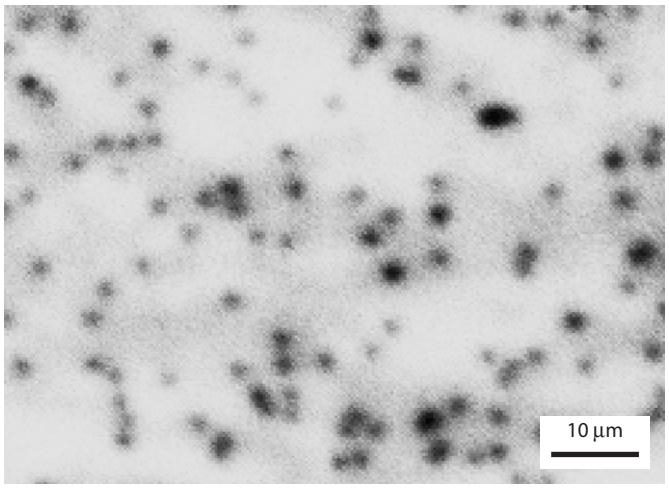

Fig. 4. Panchromatic CL image of the Ga-face of the 2 mm bulk HVPE-GaN.

Table 1
Lattice parameters, c and a, and GaN 006 and 205 rocking curve FWHM (in arcsec) of the Ga- and N-faces of the HVPE bulk GaN

	c (Å)	a (Å)	$FWHM_{006}$	$FWHM_{205}$
Ga face	5.18523 ± 0.00002	3.18926 ± 0.00004	30	25
N-face	5.18528 ± 0.00002	3.18915 ± 0.00003	70	45

establishing the lattice parameters of bulk GaN fabricated by HVPE.

3.2. Lattice parameters

3.2.1. Measuring procedure

The c and a lattice parameters of GaN were determined from the symmetric 002, 004 and 006 and asymmetric 104, 105, 204 and 205 $2\theta-\omega$ HRXRD spectra. The symmetric and asymmetric scans were measured each at four and six azimuthal positions, respectively [19]. The lattice plane spacing d^e_{hkl} is derived from the Bragg angle θ_{hkl} for every reflection using Bragg's law and taking into account the refraction correction [33]. The lattice parameters c and a were obtained from the weighted nonlinear least-squares fit of $1/(d^e_{hkl})^2$ to the following equation:

$$\left(\frac{1}{d_{hkl}}\right)^2 = \frac{4}{3}\left(\frac{h^2+k^2+hk}{a^2}\right)+\frac{l^2}{c^2}, \quad (1)$$

where d_{hkl} is the lattice spacings of a hexagonal crystal. The error Δd_{hkl}:

$$(\Delta d_{hkl})^2 = \left(\frac{\cos(\theta)\cdot\lambda\cdot\Delta\theta}{2*\sin^2(\theta)}\right)^2+\left(\frac{\Delta\lambda}{2\sin(\theta)}\right)^2, \quad (2)$$

is propagated to obtain the error of $1/d^2_{hkl}$, which is used to weigh the contribution of each reflection to the fit. In Eq. (2) λ is the X-ray radiation wavelength, θ_{hkl} is the angular position of the respective symmetric or asymmetric peak, $\Delta\theta$ is 15(6) arcsec, and $\Delta\lambda$ is 3.7×10^{-4} (3×10^{-4}) depending on the optics used.

3.2.2. HVPE-bulk GaN

The values of the lattice parameters and their errors for the Ga- and N-faces of the bulk HVPE-GaN sample are summarized in Table 1, together with the FWHM of representative symmetric (0 0 6) and asymmetric (2 0 5) rocking curves. The lattice parameters of the two faces are very close to each other, with the c-lattice parameter of the N-face slightly larger, and the a-lattice parameter slightly smaller than the respective counterparts of the Ga-face. These subtle differences are, however, statistically significant and may be explained by polishing induced changes in the lattice parameters. This speculation is supported by the larger rocking curve widths of both symmetric and asymmetric peaks for the N-face compared to the Ga-face

(Table 1), which may be attributed to polish-induced damage.

To enable comparison with existing literature data our results about the lattice parameters are plotted in Fig. 5 together with the lattice parameters of HVPE FS GaN material [19,23], HP-bulk GaN [15,21], homoepitaxial GaN grown on top of HP-bulk GaN [14,15] and GaN powder [34]. Our lattice parameters are consistent with the previously published results for FS material fabricated by HVPE. It is seen that the lattice parameters of all HVPE samples form a distinct group (marked by a rectangular box in Fig. 5), well separated from the lattice parameters of the HP bulk and homoepitaxial GaN. The lattice parameters of GaN powder [34] (which cannot sustain any microstrains) also belong to this group. The slight differences between the lattice parameters of the HVPE samples may be due to the different nucleation schemes or thickness [19]. It has been previously suggested that HVPE-GaN on sapphire is under tensile strain at the growth temperature [18], similar to MOVPE GaN layers on sapphire [35]. This so-called intrinsic growth strain is proposed to originate from grain coalescence during growth [36] and its value may differ depending on the particular nucleation scheme used and growth peculiarities.

Another reason for the observed fluctuations in the lattice parameters of the HVPE-GaN (Fig. 5) may be related to the measuring procedure involved. In some instances, HVPE samples may contain several domains that are slightly tilted to each other, and special care should be taken that one probes the same domain when measuring different reflections. Even for a single-domain GaN material (as is the case for the 2 mm thick sample studied here), the proper alignment before each $2\theta/\omega$ scan is essential. For instance, if the GaN 002 reflection is taken as an example, the c lattice parameter may deviate up to 0.0014 Å depending on the misalignment. The lattice parameters of the 2 mm bulk GaN reported in this work (Table 1) are determined from a large number of reflections and sample positions ensuring high precision, much better than previously reported (see the error bars in Fig. 5). It is important also to weigh the contribution of each reflection when fitting for the lattice parameters as described above, since the difference between the relative precision of the interplanar spacings ($\Delta d/d$) may be as large as 32% depending on the reflections used. Note that the small errors of the lattice parameters of the 2 mm-thick bulk GaN (Table 1) also reflect high in-depth and in-plane homogeneity. In view of the above discussion and the superior material properties of the 2 mm bulk GaN sample studied in this work we may then infer that its lattice parameters, $c = 5.18523$ Å and $a = 3.18926$ Å may be taken as representative for state-of-the-art (undoped) bulk GaN fabricated by HVPE.

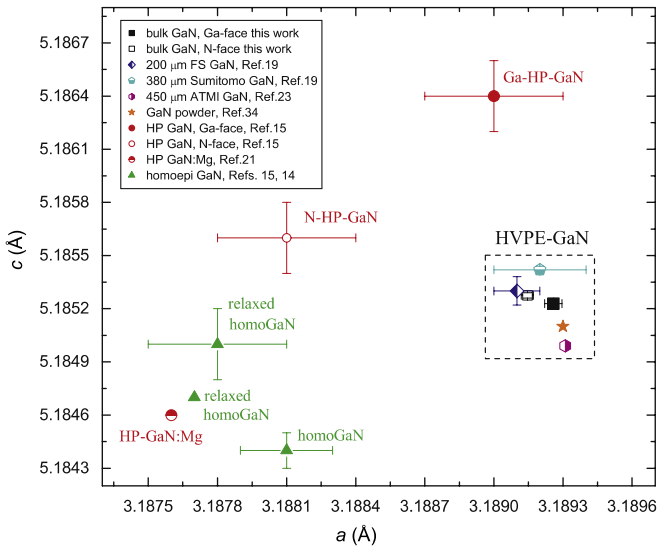

Fig. 5. Lattice parameters a and c for bulk and free-standing (FS) GaN fabricated by HVPE, HP bulk GaN and homoepitaxial GaN layer.

3.2.3. Comparison with HP bulk GaN

The two types of HP bulk material: unintentionally doped with free-electron concentration $\sim 5 \times 10^{19}$, HP-GaN, and high-resistivity GaN grown from Ga:Mg solution, HP-GaN:Mg, exhibit lattice parameters that significantly differ from those of the HVPE bulk GaN (Fig. 5). Both c and a lattice parameters of the highly conductive HP-GaN are larger compared to those of the highly resistive HP-GaN:Mg. This difference may be attributed to expansion of the HP-GaN lattice related to the high free-electron concentration due to O incorporation in the material during growth. On the other hand, the deformation potential effect cannot be evoked to explain the difference between the lattice parameters of HP- and HVPE-GaN since the free-carrier concentration in the latter is well below 10^{17} cm^{-3}. Due to the low ionization energy all O and Si donors are expected to be electrically active, and therefore the free-carrier concentration can be taken as a good estimate of the total donor impurity concentration. Consequently, the size effect related to Si and O impurities may also be readily excluded to affect the lattice parameters of the HVPE-GaN in a measurable way [14]. Surprisingly, the a lattice parameter of the HVPE bulk GaN appears to be larger than that of the highly conductive HP-GaN by 0.00026 Å (Fig. 5). The size effect related to O impurities and native defects in the HP-GaN, such as Ga vacancies and their complex with O_N could not explain the observed difference, since they all are expected to expand the lattice. In this respect we note, that the Ga-vacancies are found to be abundant in the highly conductive HP-GaN ($\sim 10^{18}$ cm^{-3}) [37], while their concentration was reported to be 2 orders of magnitude less in HVPE-GaN with free-electron concentration $< 10^{17}$ cm^{-3} [38].

The highly resistive, HP-GaN:Mg contain high concentrations of Mg and O (both typically $\sim 10^{20}$ cm^{-3}), which should expand the lattice through the size effect if incorporated as isolated impurities [14]. However, the HP-GaN:Mg has smaller a and c lattice parameters

compared to the HVPE bulk GaN (Fig. 5). The HP-GaN:Mg has been shown to comprise 3D pyramidal defects, suggested to originate from Mg clusters [16]. These 3D pyramidal defects are empty and are expected to contract the lattice, thereby compensating the expansion due to the incorporation of O and Mg. This may provide a qualitative explanation of the observed differences between HVPE bulk GaN and highly resistive HP-GaN:Mg. However, the evaluation of the size effect for the HP-GaN:Mg may be further complicated by a possible presence of N vacancies and complexes, MgO, Mg–O–N clusters with unknown effect on the lattice parameters [14]. We also note that the size effect related to the Si impurity (typical for HVPE-GaN) is negative [14]. We may then suggest that the presence of point defects cannot alone provide a plausible explanation for the observed differences between the lattice parameters of bulk GaN grown by HP and HVPE. Similarly, the deformation potential and size effects related to common impurities cannot explain the differences in the lattice parameters of the homoepitaxial layer and HVPE bulk GaN since both have a low carrier concentration $<10^{17}\,\mathrm{cm}^{-3}$. Note that the homoepitaxial layer is strained when it is pseudomorphically grown on the HP-GaN [15]. It is plausible to estimate the strain-free lattice parameters of GaN assuming a certain relaxation for the homoepitaxial layer. However, the previously estimated relaxed lattice parameters [14,15] (also shown in Fig. 5) suffer from the uncertainties in the elastic constants and differ between each other depending on the assumption made, remaining smaller than the lattice parameters of the HVPE bulk GaN. Furthermore, homoepitaxial HVPE-GaN grown on HP-GaN was reported to have smaller lattice parameters than the HP-GaN substrate [22]. This may suggest that specific growth conditions and the choice of substrate may also affect the lattice parameters.

The relative change between the lattice parameters of the HVPE bulk and the high-(low-)conductivity HP-GaN samples is 0.008 (0.05)% for the a and $-0.02(0.01)$% for the c lattice parameter. This finding indicates an anisotropic nature of the involved effect(s) on the lattice parameters and suggests that complex or extended defects might be responsible. In this respect, we point out the superior crystal and optical quality of the HVPE-GaN bulk material. However, the dislocation density in the HVPE bulk GaN is still at least 2 orders of magnitude higher compared to the HP-GaN. In principle, interaction of point defects with dislocations may give rise to a complex/anisotropic effect on the material lattice parameters. Unfortunately, quantitative information about the effect of complexes of extended defects on the lattice parameters of GaN is lacking and it is difficult to draw firm conclusions. We note that the lattice parameters of the HVPE bulk GaN may also be affected by the intrinsic growth strain due to the epitaxial nature of the growth [36]. However, a presence of such a tensile intrinsic strain in the HVPE material may contribute but cannot explain alone the observed differences in the lattice parameters since it should lead to a contraction of the c-lattice parameter because of the biaxial nature of the strain. On the other hand, the HVPE- and HP-GaN bulk material may have different elastic properties stemming from different defect structures and growth peculiarities. Consequently, this may lead to different paths of the thermal strain relaxation in the two types of bulk GaN material during the cooling down from the growth to room temperature, possibly accounting for the observed difference in the latticeparameters.

4. Summary

In summary, we have precisely measured the lattice parameters of undoped ($N_e<5\times10^{16}\,\mathrm{cm}^{-3}$) and high structural quality HVPE bulk GaN material with low density of dislocations ($N_d<6.8\pm0.6\times10^{6}\,\mathrm{cm}^{-2}$). The obtained values $c=5.18523\,\text{Å}$ and $a=3.18926\,\text{Å}$ are shown to be representative for state-of-the-art undoped bulk material fabricated by HVPE. The slight scatter in the lattice parameters observed for HVPE FS materials from different sources is attributed to a different growth strain depending on the particular nucleation scheme and growth peculiarities. A comparison between HVPE bulk GaN with HP bulk GaN, and MOVPE homoepitaxial GaN shows substantial differences in the lattice parameters of these materials. The size and deformation potential effects due to common impurities and dopants are excluded as a possible origin of the observed difference and it is suggested that a difference of the elastic properties or effect of complex or extended defects may be the reason. Further experimental and theoretical investigation are called for to unveil the origin of the observed difference in the lattice parameters of bulk GaN fabricated by different means.

Acknowledgments

V.D. would like to acknowledge valuable discussions with Prof. Z. Liliental-Weber and support from the Swedish Research Council (VR) under contract 2005-5054. We thank Dr. T. Shubina and Dr. A. Toropov for the PL measurements and Dr. A. Kakanakova for assistance with the CL measurement.

References

[1] L. Liu, J.H. Edgar, Mater. Sci. Eng. R 37 (2002) 61.
[2] B. Monemar, P.P. Paskov, J.P. Bergman, A. Toropov, T. Shubina, Phys. Status Solidi B 244 (2007) 1759.
[3] S. Porowski, I. Grzegory, J. Crystal Growth 178 (1997) 174.
[4] M. Aoki, H. Yamane, M. Shimada, T. Sekiguchi, T. Hanada, T. Yao, S. Sarayama, F.J. DiSalvo, J. Crystal Growth 218 (2000) 7.
[5] D.R. Ketchum, J.W. Kolis, J. Crystal Growth 222 (2001) 431.
[6] R. Schlesser, Z. Sitar, J. Crystal Growth 234 (2002) 349.
[7] M.K. Kelly, O. Ambacher, B. Dalheimer, G. Gross, R. Dimitrov, H. Angereer, M. Stutzmann, Appl. Phys. Lett. 69 (1996) 1749.
[8] T. Paskova, B. Monemar, in: B. Gil (Ed.), Low-dimensional Nitride Semiconductors, 2002, p. 79.

[9] C. Hemmingson, B. Monemar, Y. Kumagai, A. Koukitu, in: G. Dhanaraj, K. Byrappa, V. Prasad, M. Dudley (Eds.), Handbook of Crystal Growth, Defects and Characterization, Springer, Berlin, 2007.
[10] T. Paskova, V. Darakchieva, P. Paskov, U. Södervall, B. Monemar, J. Crystal Growth 246 (2002) 207.
[11] H. Morkoç, Mater. Sci. Eng. R 33 (2001) 135.
[12] A. Usui, H. Sunakawa, A. Yamaguchi, Jpn. J. Appl. Phys. 36 (1997) L899.
[13] J.-M. Wagner, F. Bechstedt, Phys. Rev. B 66 (2002) 115202.
[14] C.G.V. de Walle, Phys. Rev. B 68 (2003) 165209.
[15] M. Leszczynski, H. Teisseyre, T. Suski, I. Grzegory, M. Bockowski, J. Jun, S. Porowski, K. Pakula, J. Baranowski, C. Foxon, et al., Appl. Phys. Lett. 69 (1996) 73.
[16] Z. Liliental-Weber, T. Tomaszewicz, D. Zakharov, J. Jasinski, M.A. O'Keefe, Phys. Rev. Lett. 93 (2004) 206102.
[17] T. Paskova, D. Hommel, P. Paskov, V. Darakchieva, B. Monemar, M. Bockowski, T. Suski, I. Gzegory, F. Tuomisto, K. Saarinen, et al., Appl. Phys. Lett. 88 (2006) 141909.
[18] T. Paskova, V. Darakchieva, E. Valcheva, P. Paskov, I.G. Ivanov, B. Monemar, T. Böttcher, C. Roder, D. Hommel, J. Electron. Mater. 33 (2004) 389.
[19] V. Darakchieva, T. Paskova, P. Paskov, B. Monemar, N. Ashkenov, M. Schubert, J. Appl. Phys. 97 (2005) 013537.
[20] M. Leszczynski, P. Prystawko, T. Suski, B. Lucznik, J. Domagala, J. Bak-Misiuk, A. Stonert, A. Turoz, R. Langer, A. Barski, J. Alloys Compd. 286 (1999) 271.
[21] S. Porowski, J. Crystal Growth 189/190 (1998) 153.
[22] M. Krysko, M. Sarzynski, J. Domagala, I. Grzegory, B. Łucznic, G. Kamler, S. Porowski, M. Leszczynski, J. Alloys Compd. 401 (2005) 261.
[23] C. Roder, S. Einfeldt, S. Figge, D. Hommel, Phys. Rev. B 72 (2005) 085218.
[24] A. Kasic, M. Schubert, S. Einfeld, D. Hommel, T. Tiwald, Phys. Rev. B 62 (2000) 7365.
[25] M. Schubert, Infrared Ellipsometry on Semiconductor Layer Structures: Phonons, Plasmons and Polaritons, vol. 209, Springer, New York, 2004.
[26] V. Davydov, V. Emtsev, I. Goncharuk, A. Smirnov, V. Petrikov, V. Mamutin, V. Vekshin, S. Ivanov, M. Smirnov, T. Inushima, Appl. Phys. Lett. 75 (1999) 3297.
[27] V. Darakchieva, J. Birch, M. Schubert, A. Kasic, S. Tungasmita, T. Paskova, B. Monemar, Phys. Rev. B 70 (2004) 045411.
[28] F. Demangeot, J. Frandon, M. Renucci, C. Meny, O. Briot, R. Aulombard, J. Appl. Phys. 82 (1997) 1305.
[29] H. Harima, H. Sanashita, S. Nakashima, Mater. Sci. Forum 264 (1998).
[30] P. Paskov, B. Monemar, A. Toropov, J.P. Bergman, A. Usui, Phys. Status Solidi C 4 (2007) 2601.
[31] T. Metzger, R. Höpler, E. Born, O. Ambacher, M. Stutzmann, R. Stömmer, M. Schuster, H. Göbel, S. Christiansen, M. Albrecht, et al., Philos. Mag. A 77 (1998) 1013.
[32] T. Hino, S. Tomiya, T. Miyajima, K. Yanashima, S. hashimoto, M. Ikeda, Appl. Phys. Lett. 76 (2000) 3421.
[33] P.F. Fewster, N.L. Andrew, J. Appl. Cryst. 28 (1995) 451.
[34] H. Angerer, D. Brunner, F. Freudenberg, O. Ambacher, M. Stuzmann, R. Höpler, T. Metzger, E. Born, G. Dollinger, A. Bergmaier, et al., Appl. Phys. Lett. 71 (1997) 1504.
[35] S. Raghavan, J. Acord, J.M. Redwing, Appl. Phys. Lett. 86 (2005) 261907.
[36] T. Böttcher, S. Einfeldt, S. Figge, R. Chierchia, H. Heinke, D. Hommel, Appl. Phys. Lett. 78 (2001) 1976.
[37] K. Saarinen, T. Laine, S. Kuisma, J. Nissilä, P. Hautojärvi, L. Dobrzynsky, J.M. Baranowski, K. Pakula, R. Stepniewski, M. Wojdak, et al., Phys. Rev. Lett. 79 (1997) 3030.
[38] S. Hautakangas, I. Makkonen, V. Ranki, M.J. Puska, K. Saarinen, X. Xu, D.C. Look, Phys. Rev. B 73 (2006) 193301.